RSC Advances

PAPER

View Article Online
View Journal | View Issue

Cite this: *RSC Adv.*, 2021, **11**, 1360

Rapid growth of the $CH_3NH_3PbCl_3$ single crystal by microwave irradiation

Moch Wisnu Arif Sektiono, [ab] Fitri Aulia Permatasari, [a] Akfiny Hasdi Aimon[a] and Ferry Iskandar *[ac]

Received 2nd November 2020
Accepted 21st December 2020

DOI: 10.1039/d0ra09328a

rsc.li/rsc-advances

We report a rapid growth of the $CH_3NH_3PbCl_3$ single crystal through microwave irradiation. A systematic evaluation of the structural and optical properties of the obtained single crystal was also conducted. 1 minute is the optimum microwave irradiation time that generated a large single crystal of dimension (5 × 5 × 2.5) mm^3. The obtained crystal exhibits broad absorption in UV range and near-visible light luminescence under UV excitation with an optical bandgap around 2.8 eV. A fast and simple synthesis method of $CH_3NH_3PbCl_3$ single crystal with these outstanding properties could be potentially applied for any optoelectronic application with scale-up production.

Introduction

For over a decade, lots of research on the organometal trihalide perovskites (OTPs) has been conducted that focus on both the low-cost production and various superior properties. OTPs have a chemical structure of ABX_3, where A is occupied by a monovalent organic cation, B is occupied by divalent metal cations (*e.g.*, Mn^{2+}, Cu^{2+}, Pb^{2+}, Sn^{2+}), and the X site is occupied by halide elements such as I^-, Br^- or Cl^-.[1–4]

Owing to these outstanding properties, OTPs have demonstrated excellent performance in optoelectronic devices like photodetectors and solar cells.[5–7] Superior properties of OTPs including visible light absorption coefficients,[8] direct bandgap,[9,10] long carrier lifetime, and balanced exciton mobility,[11,12] strongly depend on high purity, especially crystallinity. Polycrystalline OTPs is relatively easier to be prepared by various method than the single crystal OTPs.[13] However, it suffers more limitations such as grain boundaries, voids, and defects on the surface that lead to a lower charge mobility compared to the single crystal OTPs.[14–17] A single crystal OTPs contains only one quantum well with a high order crystallization resulted in a superior optical and electrical properties compare to the polycrystalline structure.[18,19] However, in practically, the synthesis of single crystal OTPs is still challenging in various ways.

Recently, a solution growth method has been reported successfully for synthesizing the single crystal OTPs.[20,21] Dang *et al.*, successfully prepared a monocrystalline $NH(CH_3)_3SnX_3$ (X = Cl, Br) with the dimensions 13 × 8 × 6 mm^3 and 8 × 6 × 4 mm^3.[20] The crystal growth process started from immerse the crystal seed through a bottom seed solution growth (BSSG) method under atmospheric environmental condition. The morphology of the formed crystals strongly depending on the speed of tool's rotation, the orientation of the crystal seed used, and the temperature. Maculan *et al.*, prepared a $CH_3NH_3PbCl_3$ single crystal through an inverse temperature crystallization (ITC) method in oil bath resulted in $CH_3NH_3PbCl_3$ single crystals in sized 2 × 4 × 4 mm^3.[21] The ITC method requires the well-controlled of the high and continuous temperature conditions of the solution in range of 100 °C to 120 °C. Despite a large crystal size, these methods used a conduction or convection route from an external heat source then spread into a centre of sample, consuming a relatively long time crystallization process.[22]

On the other hand, microwave-assisted preparation has been reported successful to synthesize the polycrystalline OTPs films.[23,24] Contrast to conventional heating, microwave irradiation can exploit the multiple molecules in compounds (liquid, gaseous, or solid) to convert energy directly from electromagnetic to heat result in an abruptly heating process.[25] Moreover, the interaction between microwave irradiation and precursors facilitates the chemical reaction that results in a short time reaction. A microwave irradiation could then be a potential method to accelerate the crystallization process of single crystal OTPs as long a well-controlled heating rate. A microwave irradiation has also been reported successfully to promote the growth of the single crystal OTPs *i.e.*, $MAPbI_3$ and $MAPbBr_3$.[26] The low power of microwave irradiation that used led to the well-controlled temperature result in the similar crystal growth as the conventional ITC. Although the crystal growth process represents a low energy consumption, it still consumes a relatively long-time crystallization process in several hours with

[a]*Department of Physics, Faculty of Mathematics and Natural Science, Institut Teknologi Bandung, Bandung, 40132, Indonesia*

[b]*PSDKU Kediri-Politeknik Negeri Malang, Kediri, 64114, Indonesia*

[c]*Research Center for Nanosciences and Nanotechnology, Bandung, 40132, Indonesia. E-mail: ferry@fi.itb.ac.id*

a relatively smaller bulk dimension compared to the single crystal prepared from the conventional ITC method. Therefore, an exploration of an effective and efficient way for preparing the single crystal OTPs is still needed.

In this research, a rapid growth process of $CH_3NH_3PbCl_3$ single crystal through a commercial microwave preparation was conducted. The crystallization process was undergoing without the presence of the crystal seed that reduces the consuming time. A large $CH_3NH_3PbCl_3$ single crystal in a dimension of $5 \times 5 \times 2.5$ mm^3 was obtained by microwave irradiation for 1 minute time. To the best of our knowledge, a minute is the fastest for synthesizing a relatively large $CH_3NH_3PbCl_3$ single crystal. The effect of irradiation time to its crystallinity and optical properties were also investigated systematically. Thus, a commercial microwave used could reduce the crystallization time and the production cost of the single crystal OTPs' preparation.

Materials and methods

Materials

Perovskite $CH_3NH_3PbCl_3$ solution is synthesized using the wet chemical routes as reported elsewhere.[14,21] In brief, the material used as CH_3NH_3Cl salt is synthesized by reacting the hydrochloride acid solution (Merck, 37 wt% in a water solvent) and methylamine (Sigma Aldrich, 33 wt% in absolute ethanol solvent), in the absolute ethanol solvent (Merck, ≥99.5%) and under nitrogen atmospheric. 2 M solution of $PbCl_2$ powder (Sigma Aldrich, 99%) and CH_3NH_3Cl salt (1 : 1 molar ratio) in dimethyl sulfoxide or DMSO (Sigma Aldrich, anhydrous, ≥99.9%) was dissolved at 100 °C on a hotplate result in a precursor solution.

Synthesis of $CH_3NH_3PbCl_3$ single crystal

The prepared $CH_3NH_3PbCl_3$ solution was divided by 2 ml into 10 ml vials, then irradiated by a commercial microwave (Panasonic type NN-ST342M). Under a low microwave irradiation mode, the irradiation time varied from one to four minutes, resulting in single crystal samples in various dimensions. The temperature of the solution was monitored through an irradiation process by the infrared thermometer (Infrared Thermometer type GM320).

Characterizations

The crystal structure of samples was characterized by X-ray diffraction (Philips PW 1710) with Cu anode, Kα = 1.542 Å. The diffraction angle (2θ) was monitored in range of 10° into 60°. The absorption features of samples were observed by UV-Vis spectrophotometer (Ocean Optic UV-Vis spectrophotometer). The resulted absorption feature was evaluated further by using the Tauc plot to estimate the bandgap of samples. Last, the photoluminescence properties of samples were also observed by PL spectrofluorometer (RF 5300PC, Shimadzu Corp.) using Xe lamps as a light source.

Results and discussion

The samples were prepared from the precursors that consist of CH_3NH_3Cl and $PbCl_2$ as the starting materials. Microwave heating was used to accelerate the precursor's dissolution process due to the difference dielectric characteristics to the solvent in precursors. Dimethyl sulfoxide (DMSO) was selected as a solvent due to its excellent performance for dissolving CH_3NH_3Cl and $PbCl_2$.[14,21] In addition, as an aprotic polar solvent, DMSO also plays an important role in kinetic reaction owing to its high microwave absorbing feature with permittivity (ε) ≈ 47 and loss factor ($\tan\delta$) = 0.825 at the frequency of 2.45 GHz in 20 °C.[22,27,28] The commercial microwave that used can be adjusted based on two parameters, *i.e.*, duty cycle and irradiation time. The low duty cycle mode is the most reliable mode to prepare the crystal bulk since excessive evaporation has occurred when medium or high duty cycle mode was used for a minute. Then, the microwave irradiation time was varying from 1 to 4 minutes. Notably, less than 1 minute irradiation time does not generate the crystal growth and irradiation for more than 4 minutes suffer excessive evaporation that hinders the crystallization process.

Photograph of the obtained crystal samples were shown in Fig. 1. The sample was rapidly growing under a low duty cycle mode of the 800 W microwave irradiation in several minutes. It is worth pointing out that 1 minute is the fastest time to grow the crystal sample reported. Despite the other method, such as the conventional ITC method, this method does not need a crystal seed to initiate the crystal growth. The largest sample has dimension size of $5 \times 5 \times 2.5$ mm^3 obtained from 1 minute microwave irradiation. As a longer microwave irradiation time up to 4 minutes, the smaller dimension sample size was obtained. Then, the microwave irradiation time longer than 4

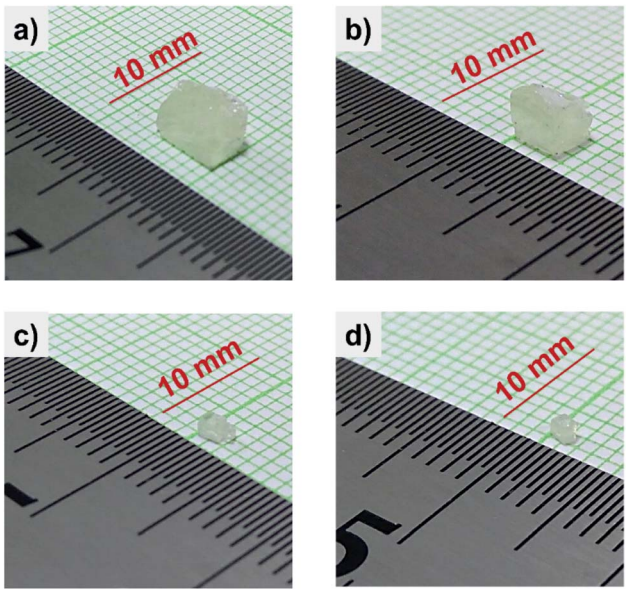

Fig. 1 Photograph taken from the as-grown $CH_3NH_3PbCl_3$ single crystal that prepared by microwave irradiation in varying irradiation time. (a) 1 minute; (b) 2 minutes; (c) 3 minutes; (d) 4 minutes.

minutes provokes the fast evaporation of precursors completely due to its high temperature.

Fig. 2a shows XRD pattern of the obtained crystal samples particulates ground from a piece of corresponding large sample. Comparing to the starting materials (CH_3NH_3Cl and $PbCl_2$), the XRD pattern of samples indicated that all samples are pure $CH_3NH_3PbCl_3$ without any residual or contaminant. All samples are pure in phase and the crystalline phase of the $CH_3NH_3PbCl_3$ perovskite, indicated by (100) and (110) planes.[31] A set of preferred orientations at 15.5°, 31.4°, and 35.2° was observed, with assigned to (100), (200) and (210) planes of the $CH_3NH_3PbCl_3$ perovskite cubic structure,[14] respectively as shown in Fig. 2b. Through a Rietveld refined data using *Pm*3*m* space group superimposed on the $CH_3NH_3PbCl_3$ as shown in Table 1, the crystal lattice constant of sample is in a reasonable value of $a = 5.6$ Å which indicated a good quality fitting and consistent with the other reports.[9,14,21,29,30] This value is also in good agreement with the estimated lattice constant value calculated based on the Bragg equation. The $CH_3NH_3PbCl_3$ that was prepared in 1 minute up to 3 minutes has the strongest peaks located at $2\theta = 15.5°$ and $2\theta = 31.4°$ that correspond to (100) and (200) planes in $CH_3NH_3PbCl_3$ crystal structure, respectively.[18] These indicated that for the samples that were prepared in 1 up to 3 minutes microwave irradiation might be dominated by the crystal in orientation of (100) and (200) planes. While for 4 minutes microwave irradiation, the crystal orientation was dominated by (110), (111), (210), (211), and (220) planes.

The optical properties of the obtained $CH_3NH_3PbCl_3$ single crystal were characterized by UV-Vis and photoluminescence spectroscopy. Fig. 3a shows the identical absorption spectrum of all $CH_3NH_3PbCl_3$ single crystal samples that were prepared in varying irradiation times. It indicates that all samples are pure $CH_3NH_3PbCl_3$ corresponds to the XRD results, as discussed in Fig. 2. The $CH_3NH_3PbCl_3$ single crystal has a clear colour showing a strong absorption a noticeably short wavelength region (<500 nm). All crystal samples also do not exhibit an absorption tail or excitonic peak indicating high quality crystal with low defect concentration.[14]

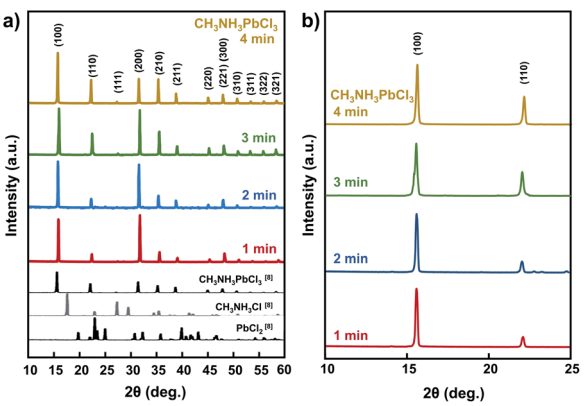

Fig. 2 X-ray diffraction patterns of the obtained single crystal samples prepared in varying microwave irradiation time. (a) Full XRD pattern; (b) zoom-in XRD pattern for $2\theta = 10–25$ degree.

Table 1 The lattice parameters of $CH_3NH_3PbCl_3$ crystals related to other research teams

Sample	Space group = $Pm\bar{3}m$, $\alpha = \beta = \gamma = 90°$, $a = b = c$ (Å)	Volume (Å^3)
Liu, Y. *et al.*, (2015)[14]	5.6855	183.783(3)
Maculan, G. *et al.*, (2015)[21]	5.67	182.284(3)
Baikie, T. et a., (2015)[9]	5.68415(6)	183.653(4)
Cheng, X *et al.*, (2018)[29]	5.6768	182.9408(9)
Nandi, P. *et al.*, (2019)[30]	5.6834	183.5797
This work (1 min)	5.6904(3)	184.2551(8)
This work (2 min)	5.6854(8)	183.77(5)
This work (3 min)	5.6827(2)	183.513(4)
This work (4 min)	5.6803(7)	183.286(5)

Surprisingly, the obtained single crystals exhibit a strong UV luminescence with peak ~340 nm under 292 nm excitation wavelength as shown in Fig. 3b. The UV luminescence was also observed on the single crystal OTPs that synthesized by other methods.[14,32,33] In varying microwave irradiation time, the PL intensity of single crystal was varying with the identical emission spectra. The single crystal prepared under 1 minute irradiation exhibits the most intense emission intensity that might be ascribed to the anisotropic crystal structure. The crystal bulk consists of the repeating atoms and the arrangements vary in different crystal orientations, which leads to an anisotropy of the crystal structure. The crystal anisotropy plays a crucial role in the optoelectronic properties in perovskite crystals. As discussed in Fig. 2b, the 1 minute sample was dominated by the (100) plane that was reported has a higher charge density than others. This charge density is related to the charge density distribution for $[CH_3NH_3]^+$ and $[PbCl_6]^{4-}$ in the crystal plane.[29] While, other samples that were dominated not only by (100) plane but also (110) plane might be suffering a great defect migration path, since the $CH_3NH_3PbCl_3$ has a pseudo-cubic structure.[34] The lattice defect because of a strong ion migration was also possibly present even though in a single crystal structure.

Fig. 4 shows a Tauc-plots that derived from the absorption spectra of $CH_3NH_3PbCl_3$ single crystal. The optical bandgap (E_g) is obtained by fitting the linear region between the axis of photon energy ($h\nu$) and the $(\alpha h\nu)^{1/n}$ with $n = 1/2$, owing to its direct bandgap properties.[14,20,35,36] Based on this approximation, the optical bandgap of the $CH_3NH_3PbCl_3$ single crystal was estimated at ~2.8 eV. This value is closed to the thin film polycrystalline perovskite (~3.1 eV) that is in the preferable range for optoelectronic application, including solar cells and field effect transistor.[33] It indicates that the obtained $CH_3NH_3PbCl_3$ single crystal could be potentially applied in the optoelectronic application.

Varying the microwave irradiation of precursor results in various dimensions of single crystal. The correlation between the sample dimension that was evaluate in volumetric crystal value with the microwave irradiation was shown in Fig. 5. The final temperature of sample right after the microwave

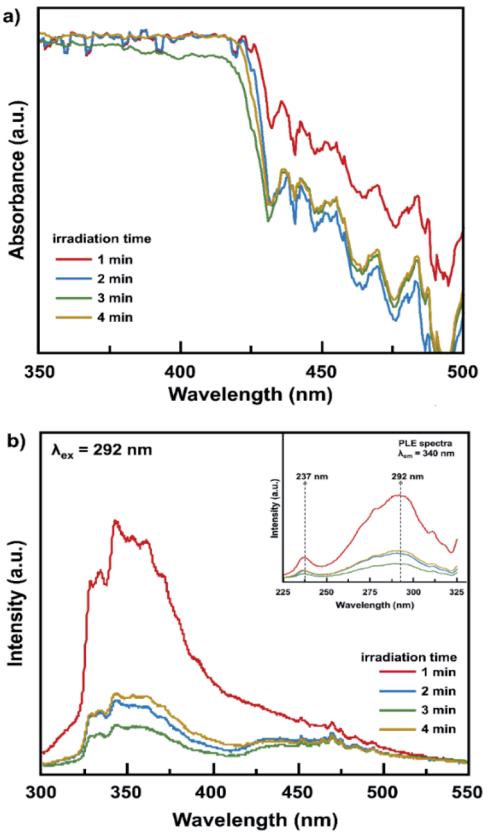

Fig. 3 Optical properties of the obtained single crystal samples that prepared in varying microwave irradiation time; (a) absorbance spectra of samples, (b) photoluminescence spectra under 292 nm excitation wavelength, right inset is PLE spectra of sample monitored at 340 nm emission wavelength.

irradiation was also presented in that figure in right *y*-axis. When the microwave irradiation time is prolonged, the single crystal size is getting smaller. Longer interaction between microwave with the precursor gives an elevated final temperature of sample. The microwave irradiation from 1 to 2 minutes gives a slightly elevated temperature of 2 °C, while the crystal size decrease significantly. It was an intriguing phenomenon since in conventional heating methods, the crystal size strongly depends on the synthesis temperature.[14,21] Thus, the possible mechanism of crystallization process might be also differing from the conventional heating.

As a comparison, several $CH_3NH_3PbCl_3$ single crystal that have been prepared by other methods were summarized in Table 2. In conventional heating, a crystal seed was required to preserve the crystal growth process *via* a first-order mechanism to the crystal seed surface.[14,29] The crystal seed was prepared from a precursor solution through conventional heating for several hours at high temperatures (*i.e.*, 80 and 100 °C). The nucleation process of crystal seed was controlled by the temperature and precursor concentration. Since the perovskite has inversely dissolution temperature characteristic, the crystal seed was limited only to the small size seed. Then, the obtained single crystal was strongly depending on the crystal seed's

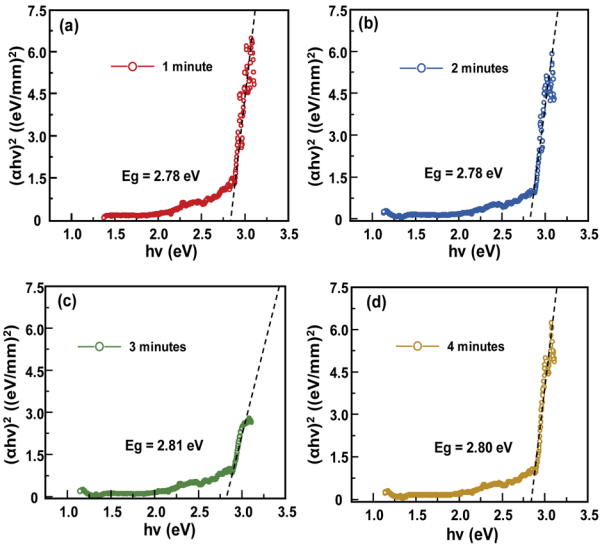

Fig. 4 Tauc-plots obtained from the absorbance spectra of samples. The intercept dash line with the horizontal axis estimate the optical band gap energy of samples.

surface area itself. While the inverse temperature crystallization method utilizes the room temperature as a growth crystal environment condition from a prepared single crystal seed.[21,41] Even though the crystal seed process took place under a lower temperature than the conventional heating, the crystal growth process took a set of repeated crystallization processes for a long time, up to several weeks. It might correspond to the slow kinetic crystal growth process under room temperature. Despite of both methods, the solvent evaporation method that was proposed by Nandi *et al.*, did not required a crystal seed.[30] The nucleation was initiated along the evaporation of precursors solution under room temperature. Thus, several weeks was required to obtain the $CH_3NH_3PbCl_3$ single crystal with the dimension of 8 × 5 × 1 mm. Regardless of the single crystal dimension, this microwave method successfully obtained a single crystal in noticeably short time without involving the

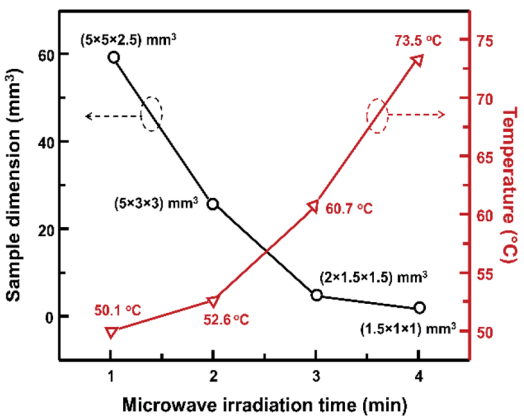

Fig. 5 The dependence of the sample dimension to the microwave irradiation time and the sample temperature right after microwave irradiation.

Table 2 Summarize of the $CH_3NH_3PbCl_3$ single crystal that were prepared by various methods

Preparation method	$CH_3NH_3PbCl_3$ single crystal dimension (in mm)	Required seed crystal	Crystal growth duration	Ref.
Conventional heating	(13.5 × 13.5 × 4.5)	Yes	100 °C, 72 h	Liu *et al.*[14]
Conventional heating	(5 × 5 × 2)	Yes	80 °C, 6–7 days	Cheng *et al.*[29]
Inverse temperature crystallization (ITC)[a]	(2 × 4 × 4)	Yes	50 °C, 6h	Maculan *et al.*[21]
Modified inverse temperature crystallization (M-ITC)[b]	(6 × 6 × 2)	Yes	20–60 °C, 5h	Chen. *et al.*[41]
Solvent evaporation	(8 × 5 × 1)	No	Room temperature, 2 weeks	Nandi *et al.*[30]
Microwave heating	**(5 × 5 × 2.5)**	**No**	**50 °C, 1 minute**	**This work**

[a] The written of crystal growth duration of ITC methods was referred to the crystal seed preparation time. [b] The written of crystal growth duration of M-ITC methods was referred to one cycle of crystal seed preparation up to room temperature cooling process. The crystal growth took place under room temperature for a couple of days through repeated cycles.

crystal seed. It suggested that this method could meet the large-scale production requirement for commercial application.

Possible mechanism of crystallization process of the $CH_3NH_3PbCl_3$ crystal bulk could be considered based on the classical nucleation theory, which explains three consecutive steps of the crystallization process, namely supersaturation, nucleation, and growth of the solid phase.[37–39] In the initial phase, the precursors solution is converted to the supersaturation of ionic solution. A systematic experiment revealed that the optimum precursor is found to be ≈ 2 M in DMSO that was also observed in other repots.[14,21] When microwave irradiation started, an elevated temperature of solution led to the dissolution of complex compounds increase of ion concentrations ($CH_3NH_3^+$, Pb^{2+}, and Cl^-) and acid content of the ionic solution.[40] This resulted ionic solution perform an efficient microwave absorption owing to its high ionic conductivity and polarizability and subsequently, the nucleation process was initiated.[22,25]

The possible mechanism of nucleation and growth process of $CH_3NH_3PbCl_3$ single crystal by microwave irradiation was proposed in Fig. 6a shows. The nucleation stage of the crystal

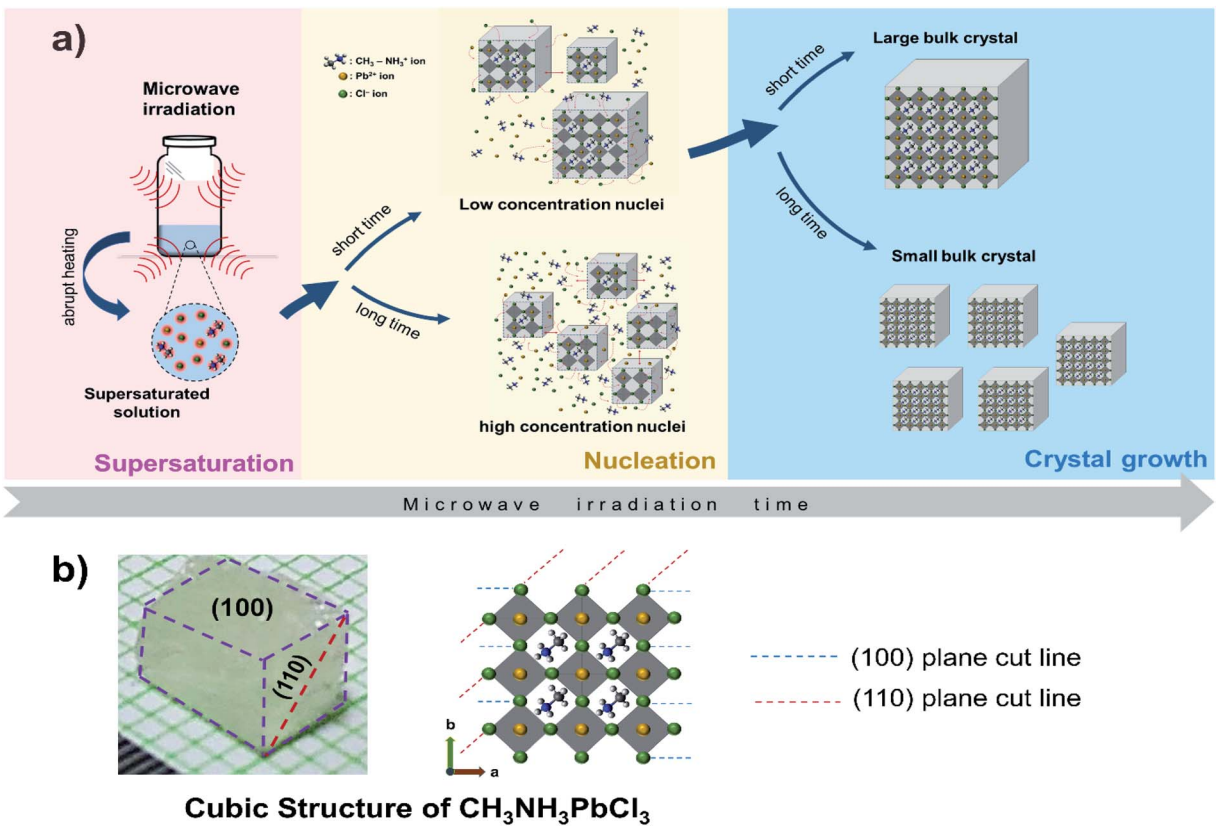

Fig. 6 (a) The schematic crystallization mechanism of $CH_3NH_3PbCl_3$ perovskite under microwave irradiation. (b) Schematic representation of plane direction based on (100) and (110) networks, obtained from cut line of the parent $CH_3NH_3PbCl_3$ cubic structure.

was generated by an abrupt supersaturation through a microwave irradiation. Short time irradiation (1 minute) gives an elevated solution temperature only up to ~50 °C that might be drift the low resulted nuclei concentration. In contrast, the longer evaporation was occurred when medium or high duty cycle mode was used for a minute. Then, the microwave irradiation time was varying from 1 to 4 minutes. Notably, less than 1 minute irradiation time do not generate the crystal growth and irradiation for more than 4 minutes suffer excessive evaporation that hinder the crystallization process irradiation time (up to 4 minutes) give an elevated solution temperature up to ~70 °C that could possibly generate more nuclei. Subsequent growth of nuclei could depend on its nuclei diffusion that correspond to the provide energy from microwave irradiation. Naturally, the low concentration of resulted nuclei could harvest a larger crystal than a high concentration of nuclei. The nucleation and growth process could possibly inhomogeneous correspond to the abrupt supersaturation during microwave irradiation.

Based on the XRD results, the resulted $CH_3NH_3PbCl_3$ single crystal could be anisotropically growing in two major directions, *i.e.* (100) and (110).[31] Fig. 6b shows the possible crystal orientation of the $CH_3NH_3PbCl_3$ single crystal that was prepared by 1 minute microwave irradiation time. This crystal was dominated by (100) plane that might be originated from strong interaction between $[CH_3NH_3]^+$ and $[PbCl_6]^{4-}$ ions. The $[CH_3NH_3]^+$ ions rotate disorderly in the ab plane and over four similar orientations in the form of the orthorhombic phase and subsequently directed towards the distorted cubic faces in the direction of (100), (010) and (001) plane.[42]

The $CH_3NH_3PbCl_3$ single crystal has highly potential application in various applications including photovoltaics, LEDs, lasers, photodetectors and other optoelectronic devices.[5,14,26] It is worth to note that the $CH_3NH_3PbCl_3$ single crystal with the (100) and (110) planes orientations exhibits superior optoelectronical properties compare to other crystal orientation, especially for the photodetector application. Owing to its anisotropic properties, the (100) planes was reported to possesses stronger charge transportation capacity than other orientation.[29] It was led by the high charge density of (100) plane that is attributed to the higher distribution density of $[CH_3NH_3]^+$ ions and $[PbCl]^-$ ions. In addition, the electron excitation energy in (100) plane lies on wide range and resulted high photocurrents. Thus, it was implied that the obtained $CH_3NH_3PbCl_3$ single crystal by microwave heating method was highly potential applied as a photodetector with excellent performances.

Conclusions

In summary, the $CH_3NH_3PbCl_3$ perovskite single crystal has been successfully synthesized through microwave irradiation in a short time. The crystal size could be well controlled by adjusting the microwave irradiation time. Short microwave irradiation time could possibly generate a low nuclei concentration result in a large crystal size. The XRD characterization of the resulted crystal indicates the as-grown crystal are in cubic phase of $CH_3NH_3PbCl_3$ with a lattice constant of $a = 5.6$ Å. The obtained crystal also exhibits broad absorption and a strong luminescence in near-visible light range under UV excitation. The Tauc-plots of the absorption spectra estimate the optical bandgap of the resulted crystal is around 2.8 eV. These outstanding properties of the $CH_3NH_3PbCl_3$ single crystal generating by short time microwave irradiation could be potentially applied in any optoelectronic application. Moreover, a simple apparatus, commercially microwave that used open the development of an efficient perovskite single crystal preparation method for scale-up production.

Conflicts of interest

There are no conflicts to declare.

Acknowledgements

F. A. P would like to thank Ministry of Finance Secretary General Indonesia Endowment Fund for Education (LPDP) for the doctoral scholarship. This work was supported by World Class University Institut Teknologi Bandung (WCU ITB) through Program Penelitian Luar Negeri Fiscal Year 2020.

References

1 G. Kieslich, S. Sun and A. K. Cheetham, *Chem. Sci.*, 2014, **5**, 4712–4715.
2 B. Saparov and D. B. Mitzi, *Chem. Rev.*, 2016, **116**, 4558–4596.
3 G. F. Needham, R. D. Willett and H. F. Franzen, *J. Phys. Chem.*, 1984, **88**, 674–680.
4 D. Weber, *Z. Naturforsch., B: J. Chem. Sci.*, 1978, **33**, 1443–1445.
5 M. I. Saidaminov, V. Adinolfi, R. Comin, A. L. Abdelhady, W. Peng, I. Dursun, M. Yuan, S. Hoogland, E. H. Sargent and O. M. Bakr, *Nat. Commun.*, 2015, **6**, 8724.
6 M. D. Birowosuto, D. Cortecchia, W. Drozdowski, K. Brylew, W. Lachmanski, A. Bruno and C. Soci, *Sci. Rep.*, 2016, **6**, 37254.
7 M. A. Green and T. Bein, *Nat. Mater.*, 2015, **14**, 559–561.
8 S. De Wolf, J. Holovsky, S.-J. Moon, P. Löper, B. Niesen, M. Ledinsky, F.-J. Haug, J.-H. Yum and C. Ballif, *J. Phys. Chem. Lett.*, 2014, **5**, 1035–1039.
9 T. Baikie, Y. Fang, J. M. Kadro, M. Schreyer, F. Wei, S. G. Mhaisalkar, M. Graetzel and T. J. White, *J. Mater. Chem. A*, 2013, **1**, 5628.
10 T. Wang, B. Daiber, J. M. Frost, S. A. Mann, E. C. Garnett, A. Walsh and B. Ehrler, *Energy Environ. Sci.*, 2017, **10**, 509–515.
11 S. D. Stranks, G. E. Eperon, G. Grancini, C. Menelaou, M. J. P. Alcocer, T. Leijtens, L. M. Herz, A. Petrozza and H. J. Snaith, *Science*, 2013, **342**, 341–344.
12 G. Xing, N. Mathews, S. Sun, S. S. Lim, Y. M. Lam, M. Gratzel, S. Mhaisalkar and T. C. Sum, *Science*, 2013, **342**, 344–347.
13 J. Chen, S. Zhou, S. Jin, H. Li and T. Zhai, *J. Mater. Chem. C*, 2016, **4**, 11–27.

14 Y. Liu, Z. Yang, D. Cui, X. Ren, J. Sun, X. Liu, J. Zhang, Q. Wei, H. Fan, F. Yu, X. Zhang, C. Zhao and S. F. Liu, *Adv. Mater.*, 2015, **27**, 5176–5183.
15 G.-J. A. H. Wetzelaer, M. Scheepers, A. M. Sempere, C. Momblona, J. Ávila and H. J. Bolink, *Adv. Mater.*, 2015, **27**, 1837–1841.
16 A. Mei, X. Li, L. Liu, Z. Ku, T. Liu, Y. Rong, M. Xu, M. Hu, J. Chen, Y. Yang, M. Gratzel and H. Han, *Science*, 2014, **345**, 295–298.
17 Y. Shao, Z. Xiao, C. Bi, Y. Yuan and J. Huang, *Nat. Commun.*, 2014, **5**, 1–7.
18 X. Chi, K. Leng, B. Wu, D. Shi, Y. Choy, Z. Chen, Z. Chen, X. Yu, P. Yang, Q.-H. Xu, T. C. Sum, A. Rusydi and K. P. Loh, *Adv. Opt. Mater.*, 2018, **6**, 1800470.
19 K. Leng, W. Fu, Y. Liu, M. Chhowalla and K. P. Loh, *Nat. Rev. Mater.*, 2020, **5**, 482–500.
20 Y. Dang, C. Zhong, G. Zhang, D. Ju, L. Wang, S. Xia, H. Xia and X. Tao, *Chem. Mater.*, 2016, **28**, 6968–6974.
21 G. Maculan, A. D. Sheikh, A. L. Abdelhady, M. I. Saidaminov, M. A. Haque, B. Murali, E. Alarousu, O. F. Mohammed, T. Wu and O. M. Bakr, *J. Phys. Chem. Lett.*, 2015, **6**, 3781–3786.
22 C. O. Kappe, *Angew. Chem., Int. Ed.*, 2004, **43**, 6250–6284.
23 Q. Cao, S. Yang, Q. Gao, L. Lei, Y. Yu, J. Shao and Y. Liu, *ACS Appl. Mater. Interfaces*, 2016, **8**, 7854–7861.
24 T. Kollek, C. Fischer, I. Göttker-Schnetmann and S. Polarz, *Chem. Mater.*, 2016, **28**, 4134–4138.
25 M. Bhattacharya and T. Basak, *Energy*, 2016, **97**, 306–338.
26 J. Jancik, A. Jancik Prochazkova, M. C. Scharber, A. Kovalenko, J. Másilko, N. S. Sariciftci, M. Weiter and J. Krajcovic, *Cryst. Growth Des.*, 2020, **20**, 1388–1393.
27 Z. Lu, E. Manias, D. D. Macdonald and M. Lanagan, *J. Phys. Chem. A*, 2009, **113**, 12207–12214.
28 Q. Jie and J. Guo-Zhu, *J. Phys. Chem. A*, 2013, **117**, 12983–12989.
29 X. Cheng, L. Jing, Y. Zhao, S. Du, J. Ding and T. Zhou, *J. Mater. Chem. C*, 2018, **6**, 1579–1586.
30 P. Nandi, C. Giri, D. Swain, U. Manju and D. Topwal, *CrystEngComm*, 2019, **21**, 656–661.
31 S. Sun, Y. Fang, G. Kieslich, T. J. White and A. K. Cheetham, *J. Mater. Chem. A*, 2015, **3**, 18450–18455.
32 L. Dimesso, M. Dimamay, M. Hamburger and W. Jaegermann, *Chem. Mater.*, 2014, **26**, 6762–6770.
33 N. Kitazawa, Y. Watanabe and Y. Nakamura, *J. Mater. Sci.*, 2002, **37**, 3585–3587.
34 Z. Zuo, J. Ding, Y. Zhao, S. Du, Y. Li, X. Zhan and H. Cui, *J. Phys. Chem. Lett.*, 2017, **8**, 684–689.
35 S. Tsunekawa, T. Fukuda and A. Kasuya, *J. Appl. Phys.*, 2000, **87**, 1318–1321.
36 J. Tauc, *Mater. Res. Bull.*, 1968, **3**, 37–46.
37 L. L. Regel and W. R. Wilcox, *Cryst. Growth Des.*, 2005, **5**, 1657.
38 K. J. Laidler and M. C. King, *J. Phys. Chem.*, 1983, **87**, 2657–2664.
39 A. A. Zhumekenov, V. M. Burlakov, M. I. Saidaminov, A. Alofi, M. A. Haque, B. Turedi, B. Davaasuren, I. Dursun, N. Cho, A. M. El-Zohry, M. De Bastiani, A. Giugni, B. Torre, E. Di Fabrizio, O. F. Mohammed, A. Rothenberger, T. Wu, A. Goriely and O. M. Bakr, *ACS Energy Lett.*, 2017, **2**, 1782–1788.
40 P. K. Nayak, D. T. Moore, B. Wenger, S. Nayak, A. A. Haghighirad, A. Fineberg, N. K. Noel, O. G. Reid, G. Rumbles, P. Kukura, K. A. Vincent and H. J. Snaith, *Nat. Commun.*, 2016, **7**, 13303.
41 Y. Chen, X. Hou, S. Tao, X. Fu, H. Zhou, J. Yin, M. Wu and X. Zhang, *Chem. Commun.*, 2020, **56**, 6404–6407.
42 M. T. Weller, O. J. Weber, P. F. Henry, A. M. Di Pumpo and T. C. Hansen, *Chem. Commun.*, 2015, **51**, 4180–4183.